# Vesicles in solutions of hard rods

B. Groh
*FOM Institute for Atomic and Molecular Physics, Kruislaan 407, 1098 SJ Amsterdam, The Netherlands*
(Received 19 November 1998)

The surface free energy of ideal hard rods near curved hard surfaces is determined to second order in curvature for surfaces of general shapes. In accordance with previous results for spherical and cylindrical surfaces it is found that this quantity is nonanalytical when one of the principal curvatures changes signs. This prohibits writing it in the common Helfrich form. It is shown that the nonanalytical terms are the same for any aspect ratio of the rods. These results are used to find the equilibrium shape of vesicles immersed in solutions of rodlike (colloidal) particles. The presence of the particles induces a change in the equilibrium shape and a shift of the prolate-oblate transition in the vesicle phase diagram, which are calculated within the framework of the spontaneous curvature model. As a consequence of the special form of the energy contribution due to the rods, these changes cannot be accounted for by a simple rescaling of the elastic constants of the vesicle as for solutions of spherical colloids or polymers. [S1063-651X(99)09704-4]

PACS number(s): 82.70.−y, 68.10.Cr, 87.16.−b, 62.20.Dc

## I. INTRODUCTION

Recently, Yaman *et al.* [1,2] obtained the surprising result that the surface tension $\gamma$ of a fluid of thin hard rods at a spherical or cylindrical wall of radius $R$ is nonanalytical at curvature $c=1/R=0$. They found different expressions for $\gamma(c)$ for positive and negative curvatures. This analysis that assumed ideal particles has been extended by Groh and Dietrich [3] by taking into account the interactions between the particles. This leads to a substantial change of the curvature dependence at medium and high particle densities, but a small singular contribution probably still remains. In the present work we return to the ideal limit but generalize the problem in two respects. First, we explicitly study arbitrarily shaped surfaces with locally varying curvatures. This is especially important because due to the mentioned singularity the curvature dependence of the surface free energy cannot have the common Helfrich form [4]. Therefore, it is not possible to derive the general expression from the special cases of spherical and cylindrical surfaces. Indeed, we find different analytical expressions depending on the signs of the local curvatures that take on an unexpected form especially at hyperbolic points. Second, we allow for a finite thickness of the rodlike particles, with the known result for spherical particles included as a limiting case.

One might ask if and how the curvature dependent surface free energy is experimentally accessible. This is indeed the case for surfaces that are free to adjust their curvature to the conditions provided by the surrounding liquid. Such surfaces are given by vesicles that consist of closed liquid bilayer membranes in an aqueous solution. Their shapes are experimentally observable by phase-contrast microscopy [5]. Theoretically, vesicles are commonly modeled as two-dimensional continuum surfaces with bending elasticity. In the simplest model the elastic energy of the membrane just has the Helfrich form. Different classes of equilibrium shapes have been determined as local energy minima (for some especially interesting examples, see Ref. [6]). For the most relevant parameter ranges the corresponding phase diagram has been worked out in detail [7].

The presence of other particles in the solution gives rise to an additional energy contribution. Due to a change of the effective spontaneous curvature the vesicle may tend to bend toward or away from the solute particles. The effects of absorbed and free polymers and of spherical colloidal particles have been reviewed by Lipowsky *et al.* [8]. Here we study the corresponding problem for rodlike particles. In contrast to the other cases, here the total elastic energy including the solute effects no longer has the Helfrich form. Thus new equilibrium shapes arise and the phase diagram is modified in a way that cannot be reduced to a simple renormalization of the parameters.

## II. SURFACE FREE ENERGY AT ARBITRARILY SHAPED WALLS

We study a system of hard spherocylinders of length $L$ and diameter $D$ in the presence of a hard wall of general shape whose principal radii of curvature $R_1$ and $R_2$ are large compared to $L$ and $D$. The interactions between the rodlike particles are neglected, i.e., we consider the dilute limit. In this section we calculate the surface free energy of the rods, which is then used in the second part of the paper to determine equilibrium shapes of vesicles immersed in the rod solution.

Using density-functional theory it can easily be shown [2] that the surface contribution $\Omega_s$ to the grand-canonical potential of the fluid is given by

$$\beta\Omega_s=\frac{\rho_b}{4\pi}\int d^3r\, d\omega\left(1-\frac{4\pi\hat{\rho}(\mathbf{r},\omega)}{\rho_b}\right), \tag{1}$$

where $\hat{\rho}(\mathbf{r},\omega)$ denotes the density of rods whose center of mass is at the point $\mathbf{r}$ and whose orientation is $\omega=(\theta,\phi)$, and $\rho_b$ is the particle density of the bulk fluid far away from the wall. Due to the hard wall potential, $n(\mathbf{r},\omega) := 4\pi\hat{\rho}(\mathbf{r},\omega)/\rho_b$ has either the value 0 or 1, depending on whether the configuration $(\mathbf{r},\omega)$ is forbidden by the presence of the surface or not. The ideal particles we assumed only

 

''feel'' the wall within a layer of thickness $(L+D)/2$ so that the spatial integration in Eq. (1) can be restricted to this layer. We introduce a local coordinate system at each point of the surface whose $z$ axis points along the normal direction into the rod solution, and whose $x$ and $y$ axes are aligned with the principal directions. As we are only interested in the leading terms in the curvature we approximate the position of the surface by

$$z_s = -\frac{1}{2}\left(\frac{x^2}{R_1}+\frac{y^2}{R_2}\right), \tag{2}$$

where we introduced the convention that a curvature $c_i = 1/R_i$ is positive if the surface curves *away* from the fluid. Now $\Omega_s$ can be written as a surface integral over the free energy density $\omega_s$:

$$\Omega_s = \int dS\, \omega_s(c_1,c_2), \tag{3}$$

with

$$\beta\omega_s(c_1,c_2) = \rho_b \int_0^{(L+D)/2} dz \;\; J(z,c_1,c_2) \times \frac{1}{4\pi}\int d\omega[1-n(z,c_1,c_2,\omega)]. \tag{4}$$

The Jacobian

$$J(z,c_1,c_2) = \frac{(z+R_1)(z+R_2)}{R_1R_2} = 1+(c_1+c_2)z+c_1c_2z^2 \tag{5}$$

takes into account the change of the tangential area element $dS$ with the normal distance $z$. The range of orientations $\omega$ for which the particle intersects the surface [i.e., for which $n(z,c_1,c_2,\omega)=0$] for given curvatures $c_1$ and $c_2$ and normal distance $z$ can be found by straightforward geometry.

### A. Infinitely thin rods

We first consider the limit of infinitely thin rods ($D=0$). At given azimuthal angle $\phi$ around the normal direction we determine the maximum allowed value $x_{max}$ for the cosine of the polar angle, at which the rod just touches the surface. This is a two-dimensional problem within the plane $\phi=$const that intersects the surface in the parabola $z_s = -c\rho^2$ ($\rho$ is the tangential coordinate within the plane), with

$$c = c(\phi) = c_1\sin^2\phi + c_2\cos^2\phi. \tag{6}$$

Note that $c(\phi)$ can be positive or negative depending on the signs of $c_1$ and $c_2$. Figure 1 shows that for positive curvatures there are two possibilities how the thin rod can touch the surface: tangentially for $z<z_c$ and with its end for $z>z_c$. It is easy to show that

$$x_{max} = \begin{cases} \left(1+\dfrac{1}{2cz}\right)^{-1/2} = \sqrt{2cz}+O(c^{3/2}), & z<z_c \\ -\dfrac{2}{cL}+\sqrt{1+\dfrac{8z}{cL^2}+\dfrac{4}{c^2L^2}} = \dfrac{2z}{L}+\left(\dfrac{L}{4}-\dfrac{z^2}{L}\right)c+\left(\dfrac{z^3}{L}-\dfrac{zL}{4}\right)c^2+O(c^3), & z>z_c, \end{cases} \tag{7}$$

with

$$z_c = \frac{1}{4c}(-1+\sqrt{1+c^2L^2}) = \frac{cL^2}{8}+O(c^3). \tag{8}$$

For negative curvatures the rod cannot approach the surface closer than $z_c=-cL^2/8$, so that $x_{max}=0$ for $z<z_c$ while for $z>z_c$ one has

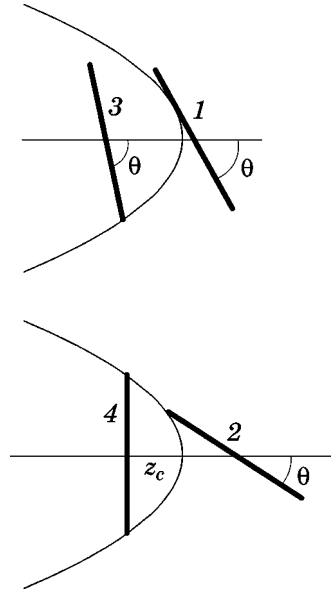


FIG. 1. Geometries for the calculation of the available orientational space of a rod near a general surface. For positive curvature the rod touches the surface tangentially for small normal distances of its center of mass (rod 1) and with its end at larger distances (rod 2). For negative curvature only end contact occurs (rod 3) and the rod cannot come closer to the surface than the distance $z_c$ (rod 4). The value of $x_{max}$ [Eqs. (7) and (9)] is the cosine of the angle $\theta$ at contact.

$$x_{max}=\frac{2z}{L}+\left(\frac{L}{4}-\frac{z^2}{L}\right)c+\left(\frac{z^3}{L}-\frac{zL}{4}\right)c^2+O(c^3) \qquad (9)$$

as before. Note that $x_{max}$ is analytic at $c=0$ only if $z>z_c$, while different expressions apply for $c\lessgtr 0$ if $z<z_c$. The surface free energy density now follows by integration over $\phi$:

$$\frac{\beta\omega_s}{\rho_b}(c_1,c_2)=\frac{1}{2\pi}\int_0^{2\pi}d\phi\int_0^{L/2}dz\;\; J(z,c_1,c_2) \times\{1-x_{max}[z,c(\phi)]\}. \qquad (10)$$

Up to terms quadratic in the curvature one obtains

$$\frac{\beta\omega_s}{\rho_b}=\frac{L}{4} \quad \text{for} \quad c_1,c_2>0 \qquad (11)$$

and

$$\frac{\beta\omega_s}{\rho_b}=\frac{L}{4}-\frac{L^3}{128}\left[(c_1+c_2)^2-\frac{4}{3}c_1c_2\right] \quad \text{for} \quad c_1,c_2<0. \qquad (12)$$

If $c_1>0$ and $c_2<0$ the function $c(\phi)$ changes sign at the angle $\phi_0=\arctan\sqrt{-c_2/c_1}$ and the $\phi$ integration must be split accordingly. After some algebra one finds

$$\frac{\beta\omega_s}{\rho_b}=\frac{L}{4}-\frac{L^3}{192\pi}[3\sqrt{-c_1c_2}(c_1+c_2) +(3c_1^2+2c_1c_2+3c_2^2)\arctan\sqrt{-c_2/c_1}] \quad \text{for} \quad c_1>0,c_2<0. \qquad (13)$$

Of course the same formula with $c_1$ and $c_2$ interchanged applies for $c_1<0$ and $c_2>0$. Thus depending on the signs of the principal curvatures, $\omega_s$ is given by Eqs. (11), (12), or (13). Equation (12) was already derived by Yaman *et al.* [see Eq. (A9) in Ref. [2]] who also showed that Eq. (11) is exact for a convex surface to all orders in the curvature. Our new result [Eq. (13)] provides a continuous connection between Eqs. (11) and (12). This is demonstrated in Fig. 2 where $\omega_s$ is plotted for $c_1=c\cos\psi$ and $c_2=c\sin\psi$ as a function of $\psi$ for fixed $c$. Obviously the presence of the rods favors surfaces with two negative principal curvatures. Terms linear in the curvature are absent in all cases. The quadratic terms are nonanalytic if one of the $c_i$'s changes sign, which, inter alia, precludes writing the curvature dependence of the surface free energy in the common Helfrich form

$$F_{Hel}=\int dS\left[\frac{1}{2}\kappa(c_1+c_2-C_0)^2+\bar{\kappa}c_1c_2\right], \qquad (14)$$

with the bending rigidities $\kappa$ and $\bar{\kappa}$ and the spontaneous curvature $C_0$. If one restricts oneself to equal signs of $c_1$ and $c_2$ we have rigorously shown here that the Helfrich form can be applied with $\beta\kappa/\rho_b=-L^3/64$ and $\beta\bar{\kappa}/\rho_b=L^3/96$ for negative and, trivially, $\kappa=\bar{\kappa}=0$ for positive curvatures. However, surfaces of vesicles typically exhibit regions with differing signs, so that a global mapping to the Helfrich form is no longer possible.

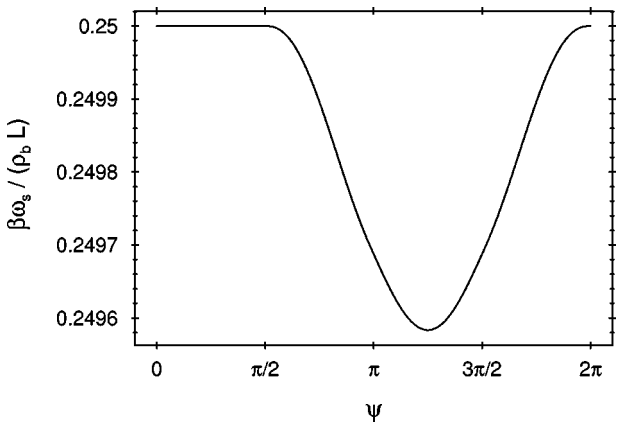


FIG. 2. Curvature dependence of the surface free energy density $\omega_s(c_1,c_2)$ for $c_1=c\cos\psi$ and $c_2=c\sin\psi$. The value of $c$ is kept fixed ($cL=0.2$) and $\psi$ is varied from 0 to $2\pi$ providing a continuous path through the four possible sign combinations of $c_1$ and $c_2$ for which four different analytical expressions [Eqs. (11)–(13)] apply. The curve is nonanalytic at $\psi=\pi/2,\pi,3\pi/2,2\pi$. The third derivative with respect to $\psi$ diverges on one side of these points.

### B. Rods of finite thickness

The case of spherocylindrical particles with finite thickness $D$ can be reduced to the problem for $D=0$ discussed above if one realizes that the surface of the spherocylinder consists of all points that have a distance $D/2$ from the line segment of length $L$, which connects the centers of the hemispherical caps. Thus if the spherocylinder touches the surface $S$ this line segment touches a parallel surface $S'$ shifted by $D/2$. The curvature radii of $S'$ and $S$ are simply related by $R_i'=R_i+D/2$, i.e., $c_i'=c_i/(1+c_iD/2)$ [9], so that for $z>D/2$,

$$n(z,c_1,c_2,D) =n[z-D/2,c_1/(1+c_1D/2),c_2/(1+c_2D/2),0]. \qquad (15)$$

The particles cannot approach the wall closer than $z=D/2$. This inaccessible range yields the $L$ independent contribution

$$\frac{\beta\omega_s^{(1)}}{\rho_b}=\int_0^{D/2}dz\;\; J(z,c_1,c_2)=\frac{D}{2}+\frac{D^2}{8}(c_1+c_2)+\frac{D^3}{24}c_1c_2 \qquad (16)$$

to the free energy density. By using the fact that

$$J(z'+D/2,c_1,c_2)=J(z',c_1',c_2')(1+c_1D/2)(1+c_2D/2), \qquad (17)$$

one obtains for the remaining $z$ integral from $D/2$ to $(L+D)/2$,

$$\omega_s^{(2)}(c_1,c_2,D)=\left(1+\frac{c_1D}{2}\right)\left(1+\frac{c_2D}{2}\right)\omega_s(c_1',c_2',0). \qquad (18)$$

Now the above results for infinitely thin rods can be employed to give the final result

$$\frac{\beta\omega_s}{\rho_b}=\frac{D}{2}+\frac{L}{4}+\left(\frac{D^2}{8}+\frac{DL}{8}\right)(c_1+c_2)+\left(\frac{D^3}{24}+\frac{D^2L}{16}\right)c_1c_2+\Delta f_s, \tag{19}$$

with

$$\Delta f_s=0, \quad c_1,c_2>0 \tag{20}$$

$$\Delta f_s=-\frac{L^3}{128}\left[(c_1+c_2)^2-\frac{4}{3}c_1c_2\right], \quad c_1,c_2<0 \tag{21}$$

$$\Delta f_s=-\frac{L^3}{192\pi}\left[3\sqrt{-c_1c_2}(c_1+c_2)+(3c_1^2+2c_1c_2+3c_2^2)\arctan\sqrt{-\frac{c_2}{c_1}}\right], \quad c_1>0, c_2<0. \tag{22}$$

It is remarkable that all the additional terms that contain powers of $D$ are analytic in $c_1$ and $c_2$. The singular contributions $\Delta f_s$ are exactly the same as in the limit $D\to 0$. In this sense no qualitatively new features arise when the thickness of the rods is taken into account. Therefore, we only consider thin rods in the second part of this paper. The special case of hard noninteracting spheres is also contained in the above analysis for $L=0$. Only in this case the full $\omega_s$ is analytic and thus lends itself to the Helfrich expansion. Our result for the spheres is in agreement with previous calculations [1,10].

We remark that the crossover between rods and polymers has been analyzed to a certain extent in Ref. [2]. These authors determined the surface free energy of segmented rods with a small number of monomers $N$ at spherical walls and found that the difference between the coefficients of the quadratic terms for positive and negative curvature becomes smaller with increasing $N$. One may speculate that this difference vanishes for $N\to\infty$, so that long polymers, like hard spheres, would represent another special case for which $\omega_s$ is analytic.

### III. VESICLE SHAPES IN A ROD SOLUTION

We now consider a vesicle immmersed in a solution of rodlike colloids. It is assumed that the rods are not absorbed on the membrane and that their interaction can be approximated by the hard wall model. The bending energy of the vesicle consists of two contributions. First, the internal bending rigidity of the membrane, which is described in the so-called spontaneous curvature model as given by Eq. (14) (For other possibilities see, e.g., [5,11]). Second, the presence of the rodlike particles gives rise to the surface free energy determined in the previous section. If the vesicle is immersed in a solution of polymers [12] or diluted spherical colloids this second contribution will have the same analytical form as the first and therefore lead to a renormalization of the rigidity coefficients and the spontaneous curvature of the ''free'' vesicle. Then the equilibrium shapes are those determined for the pure spontaneous curvature model [7] and the addition of the solute only shifts the system to a different point in the phase diagram. However, in the present case the second energy contribution, due to the rods, cannot be written in the Helfrich form so that new equilibrium shapes will arise. As shown in Sec. II B a nonzero thickness of the rods can also be taken into account by using renormalized coefficients in $F_{Hel}$. Therefore, in the following we only use the expressions for infinitely thin rods.

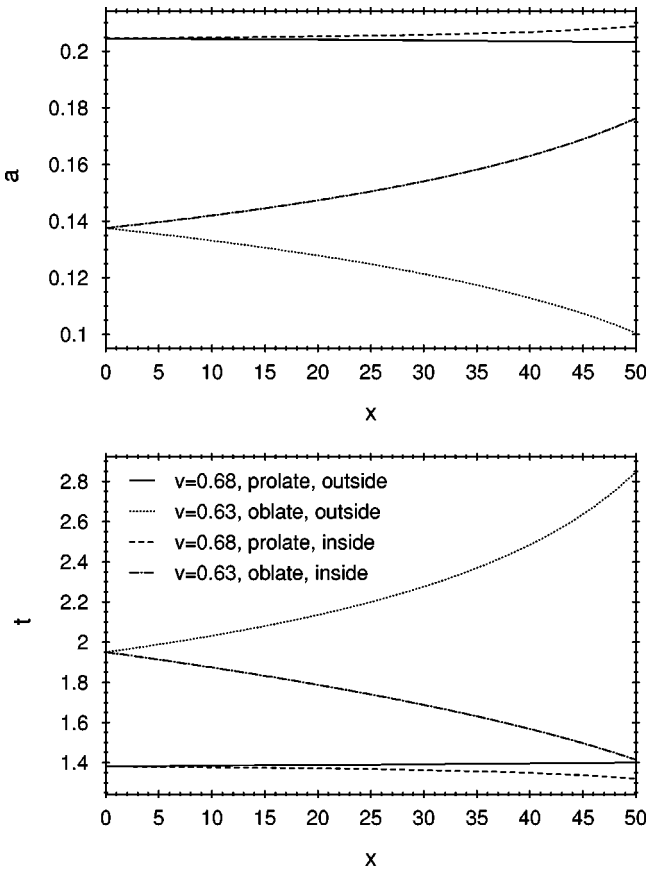


FIG. 3. Aspect ratio $a$ and bulging parameter $t$ (see main text) of the equilibrium shape as a function of the reduced concentration $x$ of rods inside and outside the vesicle for prolates and oblates at two reduced volumina $v$ close to the transition point ($c_0=0$).

Because the energy scale associated with the bending rigidity $\kappa$ is much smaller than the energies necessary to change significantly the area $A$ or the volume $V$ of the vesicles, these quantities are regarded as fixed. Thus the equilibrium shape is determined by a minimization of $F_{tot}=F_{Hel}+\Omega_s$ under the constraint of fixed $A$ and $V$. Due to the scale invariance of $F_{tot}$ the equilibrium shape depends only on the dimensionless parameters

$$v=\sqrt{36\pi}\frac{V}{A^{3/2}}, \quad c_0=C_0\sqrt{\frac{A}{4\pi}}, \quad x=\frac{\rho_b L^3}{\beta\kappa}. \tag{23}$$

A sphere is characterized by $v=1$, while for any other shape, $v<1$. The parameter $x$ measures the relative importance of the contribution $\Omega_s$ due to the rods. The Gaussian curvature term proportional to $\bar{\kappa}$ in Eq. (14) is constant for topologically equivalent shapes and will be omitted since we consider only shapes with the same topology as the sphere. We will focus on the region $v\lesssim 1$ and moderate values of $c_0$ where the equilibrium shapes of the pure spontaneous curva-

ture model are axisymmetric prolates or oblates with up-down symmetry, separated by a first-order transition [7].

Rather than deriving and solving the exact Euler-Lagrange shape equations we parametrize the surfaces by simple two-parameter functions. In cylindrical coordinates $(r,z,\phi)$ around the axis of symmetry we write [13]

$$r(z)=a\sqrt{1-z^2}\sqrt{1+bz^2} \quad \text{for prolates,} \tag{24}$$

$$z(r)=a\sqrt{1-r^2}\sqrt{1+br^2} \quad \text{for oblates.} \tag{25}$$

These shapes reduce to ellipsoids for $b=0$, while increasing the value of $b$ leads to a bulging, which finally yields nonconvex shapes for $b>1$. The parameter $a$ is the aspect ratio of the shape, i.e., the ratio of its diameter in the equatorial plane and its length along the symmetry axis (or vice versa for oblates). We emphasize that the bending energy does not depend on the size of the vesicles so that the length of one axis can be arbitrarily set to unity. The corresponding vesicle volumes are

$$V_{pro}=\frac{4\pi}{3}a^2\left(1+\frac{b}{5}\right), \tag{26}$$

$$V_{obl}=\frac{\pi a}{2b}\left[b-1+\frac{(b+1)^2}{2\sqrt{b}}\left(\frac{\pi}{2}+\arcsin\frac{b-1}{b+1}\right)\right], \tag{27}$$

and the areas

$$A_{pro}=4\pi a\int_0^1 dz\,\sqrt{(1-z^2)(1+bz^2)+a^2z^2(1-b+2bz^2)^2}, \tag{28}$$

$$A_{obl}=4\pi\int_0^1 dr\;\; r\sqrt{1+a^2r^2\frac{(1-b+2br^2)^2}{(1-r^2)(1+br^2)}}. \tag{29}$$

The principal curvatures are

$$c_1^{pro}=r(z)\sqrt{1+r'(z)^2}, \quad c_2^{pro}=-\frac{[1+r'(z)^2]^{3/2}}{r''(z)} \tag{30}$$

for prolates and

$$c_1^{obl}=-\frac{r\sqrt{1+z'(r)^2}}{z'(r)}, \quad c_2^{obl}=-\frac{[1+z'(r)^2]^{3/2}}{z''(r)} \tag{31}$$

for oblates. All curvatures are positive for $b<1$. In the prolate case $c_2^{pro}$ becomes negative for $z<z_c$, where $z_c$ is the positive solution of

$$-1+b^2z^4(-3+2z^2)+b(1-6z^2+3z^4)=0. \tag{32}$$

For oblates three ranges must be distinguished: for $r<r_{c1}$, where $r_{c1}$ is again determined by Eq. (32), both curvatures are negative. Between $r_{c1}$ and $r_{c2}=\sqrt{(b-1)/(2b)}$, $c_2^{obl}$ is positive and $c_1^{obl}$ is negative, while for $r>r_{c2}$ both curvatures are positive. The rod contribution to the elastic energy is computed from

$$\Omega_s=\int dS\;\omega_s(c_1,c_2)=\begin{cases}4\pi\displaystyle\int_0^1 dz\;\; r(z)\sqrt{1+r'(z)^2}\;\omega_s[c_1^{pro}(z),c_2^{pro}(z)], & \text{prolates}\\ 4\pi\displaystyle\int_0^1 dr\, r\sqrt{1+z'(r)^2}\;\omega_s[c_1^{obl}(r),c_2^{obl}(r)], & \text{oblates.}\end{cases} \tag{33}$$

The equilibrium shapes follow by a numerical minimization of the total elastic energy $F_{tot}[a(b,v),b]$ with respect to $b$, where $a(b,v)$ is obtained by numerical solution of the first equation of Eq. (23).

If the rods are inside instead of outside the vesicle the signs of the curvatures $c_i$ have to be reversed in the computation of $\Omega_s$. For the case of particles on *both* sides of the membrane, $\omega_s(c_1,c_2)$ must be replaced by $\omega_s(c_1,c_2)+\omega_s(-c_1,-c_2)$ which, interestingly, has the form given by Eq. (12) for *all* signs of $c_i$. Hence here the Helfrich form is valid, as has been surmised by Yaman *et al.* [1], so that for $c_0=0$ the equilibrium shape does not depend on the rod concentration $x$.

We first discuss the results for zero spontaneous curvature. If $b>1$ the shape can be characterized by a ''bulging'' parameter $t=(b+1)/2b^{1/2}$, which is equal to the ratio of the maximum of $r(z)[z(r)]$ and its value in the equatorial plane [along the symmetry axis] for prolates [oblates]. In Fig. 3 the quantities $a$ and $t$ are shown as a function of $x$ for a prolate and an oblate at $v$ values in the vicinity of the phase transition. Rods outside a prolate tend to decrease $a$ and increase $t$ thereby narrowing the waist of the vesicle. Similarly, an oblate develops stronger ''dips'' at the symmetry axis in order to increase the range and degree of negative curvature. These results confirm our previous observation that the surface prefers to bend toward the rods. Figure 4 shows some examples for shapes without and with rods outside and inside the vesicle. The changes of $a$ and $t$ are much smaller for prolates (0.4–1.3 % at $x=30$) than for oblates (10–15 %).

Identifying the most probable shape with the lowest energy shape is problematic when the energy is a nonanalytic function of the shape that might be nonquadratic for small deviations from the energy minimum [14]. However, numerically the function $\Omega_s[a(b,v),b]$ shows no traces of nonanalyticity. In fact, the integrand $\omega_s(c_1,c_2)$ is singular

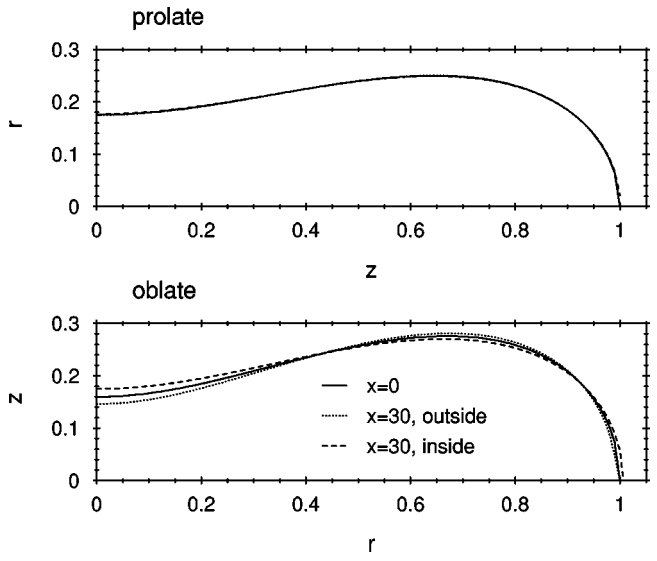


FIG. 4. Equilibrium shapes for $c_0=0$ at $v=0.648$, which corresponds to the transition point if no rods are present. Only one quarter of the contours is drawn; the remaining parts follow by symmetry. Note that the symmetry axis is drawn horizontally for the prolates and vertically for the oblates. Within each part of the figure the shapes are scaled to the same volume and area. The presence of rods outside or inside the vesicle induces a modification of the shape which for the prolates is hardly visible on this scale.

only on a set of measure zero (on the curves determined by $c_1c_2=0$) so that the singularity is probably removed by the integration.

Without rods the phase transition between prolates and oblates takes place at $v=0.648$ within our approximation, which is very close to the value $v=0.651$ obtained by an exact minimization [7]. The coexisting shapes (see Fig. 4) are both strongly nonspherical with an aspect ratio $a\simeq 0.17$, which indicates a pronounced first-order character of the transition. As shown in Fig. 5 the rods shift the transition to larger $v$ if they are outside the vesicle and to smaller $v$

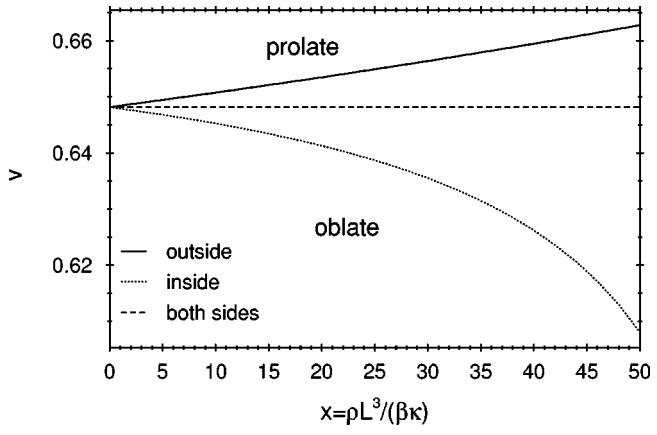


FIG. 5. Phase boundary between prolates and oblates for $c_0=0$ as a function of the dimensionless rod concentration $x$ outside, inside, or on both sides of the vesicle. Particles outside favor oblate shapes, particles inside, prolate shapes. If particles are present on both sides, their contribution to the elastic energy has the Helfrich form, too, so that the equilibrium shapes and the boundary are not altered.

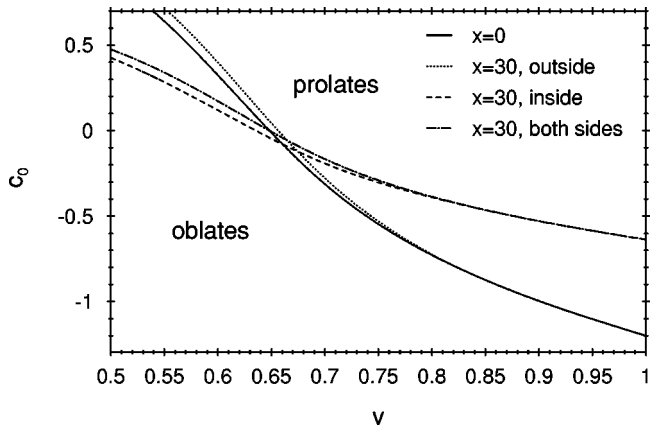


FIG. 6. Phase diagram in the $v,c_0$ plane for vesicles in the absence and presence of rods. The lines approach the maximum value $v=1$ at $c_0=-6/5$ for $x=0$ or rods outside, but at $c_0=-6/5(1-x/64)$ for rods inside or on both sides (see main text).

inside. As explained above, rods on both sides effectively just change the value of $\kappa$ but do not influence the phase diagram.

We now turn to the more general case of nonzero spontaneous curvature $c_0$. Negative values of $c_0$ favor oblate shapes so that the transition point moves to higher volume to surface ratios $v$ (Fig. 6). It has been shown rigorously that the phase boundary approaches $v=1$ at $c_0=-6/5$ [15,7]. By a series expansion of the elastic energy around $v=1$ one finds that this also holds within the present parametrization. The presence of rods outside the vesicle shifts the transition line to larger $v$. However, no shift occurs for $v>0.87$ because in this range both coexisting shapes are convex ($b<1$) so that $\Omega_s=$const. Rods on both sides of the membrane give rise to an additional Helfrich-like term with $\beta\kappa_{rod}=-\rho_b L^3/64$ and $c_{0,rod}=0$. Therefore, the effective bending rigidity is $\kappa'=\kappa+\kappa_{rod}$ and the effective spontaneous curvature is

$$c_0'=\frac{c_0}{1-x/64}. \tag{34}$$

For this reason the curve for particles on both sides differs from the curve for $x=0$ in Fig. 6 (except at $c_0=0$) and reaches $v=1$ at $c_0=-6/5(1-x/64)$, whereas both curves are identical if plotted as a function of $c_0'$ instead of $c_0$ (Fig. 7). We note that $\kappa'$ becomes negative for $x>64$. In this case the present analysis breaks down and higher order terms in the curvature must be taken into account. If the rods are restricted to the inside of the vesicle the same effective Helfrich form applies as long as only convex shapes are considered. This explains why the corresponding phase boundary is equal to that for rods on both sides at large $v$. However, for smaller $v$, shapes with differing signs of the curvatures occur that cannot be accounted for by a simple rescaling of the Helfrich coefficients and that shift the transition line in Fig. 7 to lower $v$ compared to the pure Helfrich case.

## IV. DISCUSSION

In summary, we have shown that if rodlike particles are present on the outer or inner side of a vesicle its equilibrium

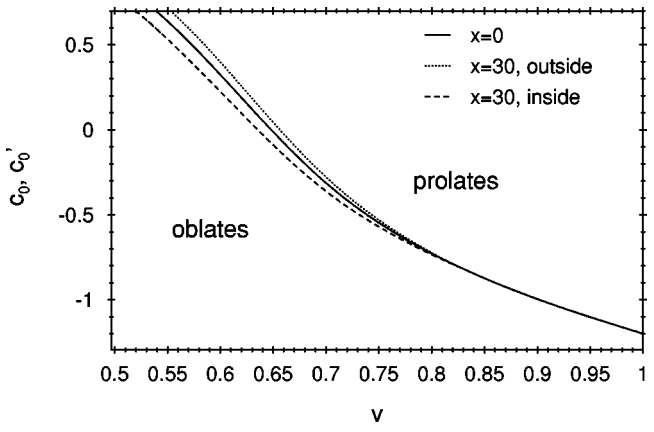


FIG. 7. Same phase diagram as in Fig. 6 but plotted in terms of the effective spontaneous curvature $c_0'$ [Eq. (34)] for rods inside and on both sides of the vesicle. The curve for the latter case coincides with that for the free vesicle ($x=0$) in this representation.

shape changes. Because the curvature dependence of the surface free energy of the solutes cannot be written in the Helfrich form their effect cannot be described by a simple rescaling of the bending rigidity coefficients. We have quantitatively computed the shape changes and the shift of the prolate-oblate transition line in the phase diagram.

In order to decide whether these effects are large enough to be observable in experiments an estimate for the quantity $x=\rho_b L^3/\beta\kappa$ is needed. The bending rigidity is typically of the order of $10^{-19}$ J [5]. If the rod density $\rho_b$ is too large the rod-rod interaction becomes important, which might screen the interesting effects [3]. Since these interactions scale with the second virial coefficient $B_2 \sim DL^2$, a useful dimensionless measure for their strength is $\rho_b^* = \rho_b DL^2$. So even if $\rho_b^*$ must be limited to a small number, 0.1 say, $x$ can in principle be made arbitrarily large by choosing large enough aspect ratios $L/D$. In practice, however, one would need $L/D \sim O(10^3)$ to obtain $x \sim O(10)$. This is much higher than for the ''classical'' rodlike colloidal particles like the tobacco mosaic virus [16] but may be achievable with microtubules for which $D=25$ nm and $L$ can be tens of micrometers. Rather large vesicles would have to be used so that the curvature radii are still large compared to $L$, which justifies the neglection of higher order terms in the curvature.

Microtubules and many other mesoscopic rodlike particles are usually polydisperse. Thus a useful extension of the present work would be the inclusion of polydispersity, which poses no fundamental technical problems as long as the interparticle interactions can still be neglected. A generalization to soft particle-wall interactions seems to be more difficult as no simple analytical expressions for more realistic potentials exist.

Finally we mention that contrary to what is claimed in Ref. [1] the corresponding problem for disks instead of rods is not completely equivalent. It is easy to convince oneself with a coin and a cup that there are configurations where a disk touches the inside of a cylinder at two isolated points whose distance is smaller than the disk diameter. The orientational constraints due to these configurations obviously cannot be described by replacing the disk with an equivalent rod.

## ACKNOWLEDGMENTS

The author thanks U. Seifert, A. Hanke, and S. Dietrich for helpful discussions, and B. Mulder and M. Bates for a critical reading of the manuscript. This work is part of the research program of the Stichting voor Fundamenteel Onderzoek der Materie (Foundation for Fundamental Research on Matter) and was made possible by financial support from the Nederlandse Organisatie voor Wetenschappelijk Onderzoek (Netherlands Organization for the Advancement of Research). The author acknowledges the financial support of the EU through the Marie Curie TMR Fellowship Program.

[1] K. Yaman, P. Pincus, and C. Marques, Phys. Rev. Lett. **78**, 4514 (1997).
[2] K. Yaman, M. Jeng, P. Pincus, C. Jeppesen, and C. Marques, Physica A **247**, 159 (1997).
[3] B. Groh and S. Dietrich, Phys. Rev. E **59**, 4216 (1999).
[4] W. Helfrich, Z. Naturforsch. C **28**, 693 (1973).
[5] H.-G. Döbereiner, E. Evans, M. Kraus, U. Seifert, and M. Wortis, Phys. Rev. E **55**, 4458 (1997).
[6] Y. Jie, L. Quanhui, L. Jixing, and O.-Y. Zhong-Can, Phys. Rev. E **58**, R4730 (1998).
[7] U. Seifert, K. Berndl, and R. Lipowsky, Phys. Rev. A **44**, 1182 (1991).
[8] R. Lipowsky, H.-G. Döbereiner, C. Hiergeist, and V. Indrani, Physica A **249**, 536 (1998).
[9] M. P. do Carmo, *Differential Geometry of Curves and Surfaces* (Prentice-Hall, Englewood Cliffs, 1976), p. 212.
[10] E. Eisenriegler, A. Hanke, and S. Dietrich, Phys. Rev. E **54**, 1134 (1996).
[11] L. Miao, U. Seifert, M. Wortis, and H.-G. Döbereiner, Phys. Rev. E **49**, 5389 (1994).
[12] A. Hanke, E. Eisenriegler, and S. Dietrich, Phys. Rev. E (to be published).
[13] K. Helal, T. Biben, and J.-P. Hansen, J. Phys. Condens. Matter **11**, L51 (1999).
[14] A. Hanke (private communication).
[15] S. Milner and S. Safran, Phys. Rev. A **36**, 4371 (1987).
[16] G. Vroege and H. Lekkerkerker, Rep. Prog. Phys. **55**, 1241 (1992).